Observing Distant Type Ia Supernovae with the ESO VLT

The discovery of the accelerating Universe through observations of distant Type Ia supernovae (SNe Ia) was one of the most exciting scientific discoveries of the past decade. The acceleration is apparently driven by a mysterious "dark" energy which overcomes the gravitational pull of matter. One of the best ways of constraining the nature of the dark energy is to build a larger, better-observed sample of distant SNe Ia over a wide range of redshifts. The Supernova Cosmology Project (SCP) has been using ESO and other telescopes to do just that and, in this article, we give an overview of the data we have collected thus far and we present some preliminary results.

Chris Lidman (ESO)
for The Supernova Cosmology Project[1]

Towards the end of the 1990's, two international collaborations independently used the apparent brightness of distant[2] Type Ia supernovae (SNe Ia) to discover that the rate of the Universe's expansion, contrary to what was then the common wisdom, is currently accelerating, and to infer that a mysterious form of energy – now called the dark energy – dominates the Universe (Riess et al. 1998; Perlmutter et al. 1999; for reviews, see Leibundgut 2001 and Perlmutter and Schmidt 2003). Since this discovery, measurements of the Cosmic Microwave Background (CMB) anisotropy, statistical analysis of galaxy redshift surveys, and measurements of the number density of massive galaxy clusters have shown that the Universe is flat and that matter, including dark matter, makes up about a quarter of the critical energy density. When these results are combined with the results from distant SNe Ia (Fig. 1), we infer that about 75% of Universe is made up of dark energy.

This is a remarkable result, and an extraordinary number of diverse theories have been proposed to explain the nature of the dark energy and the reason why it now dominates our Universe. For both matter and dark energy, the equation of state[3] relates the pressure to the energy density via

$$p = w(z)\,\rho,$$

where p is the pressure, ρ is the energy density, z is the redshift and $w(z)$ is the equation of state parameter. For non-relativistic matter, w is zero; for photons, it is 1/3; and for dark energy, it is negative. Candidates for dark energy include Einstein's cosmological constant, in which w is exactly –1, quintessence, in which it is variable and greater than –1, and other more exotic theories, such as "phantom energy" theories, in which it is less than –1. Recent results, which combine high-quality HST data of distant SNe Ia (Knop et al. 2003, Riess et al. 2004) with the data from galaxy redshift surveys and the CMB, show that it is close to –1. Is w equal to –1 and is it a constant? The answer to this question will fundamentally change the way we see our Universe.

As a tool to measure cosmological distances, SNe Ia are unique. Their peak luminosities are very uniform, which means that an accurate measure of the distance can be obtained from the apparent brightness, and they are also intrinsically very bright, so they can be observed over enormous distances. In terms of redshift, SNe Ia with redshifts as high z~1.5 are now observed. This corresponds to a time when the Universe was about one-third of its current age[4].

Although the Universe is now accelerating, this was not always the case. Up until about 5 billion years ago, the Universe was matter dominated and decelerating. The change between deceleration and acceleration occurred around z=0.5. By observing SNe Ia over a wide range of redshifts, one can get a picture of the expansion history of the Universe from just a few billion years after the big bang to today, and this includes the epochs of deceleration and acceleration.

In 2000 and following a successful pilot program that discovered a SN Ia at z=1.2 (Aldering 1998), the SCP embarked on a program to discover and follow a large number of SNe Ia over a wide range of redshifts. We use these data to extend observations of SNe Ia to redshifts greater than one, to measure the expansion history of the Universe from deceleration to acceleration, to constrain the dark energy equation of state, and to assess the importance of SN Ia evolution and extinction from dust. This program has made extensive use of ESO facilities and included spectroscopic confirmation and follow-up imaging with FORS1 and FORS2 and infra-red (IR) *J*-band imaging with ISAAC.

In this article we give an overview of how SNe Ia are discovered, we discuss the follow-up observations that we have done with the ESO VLT and we present some preliminary results. These results will appear in a series of papers, which, at the time of writing, have either been submitted or are in preparation (Lidman et al. 2004; Nobili et al. in preparation; Garavini et al. in preparation).

Search and Discovery

Starting in 2000 and ending in 2002, the SCP performed 8 separate high-redshift supernova searches involving the CFHT12k camera on CFHT, the MOSAICII camera on the CTIO Blanco telescope and Suprime-Cam on Subaru. In general, each of the searches aimed at discovering SNe Ia at different redshifts and, hence, the search areas and the search depths vary from one search to the next. For example, the 2002 CTIO search exclusively targeted SNe Ia at z~0.5, and thus searched a relatively large area of

[1] Members of the SCP are listed at the end of this article
[2] In the context of this article, we use distant to refer to supernovae that have redshifts $z > 0.1$ and nearby to refer to supernovae that have redshifts $z \leq 0.1$
[3] The equation is written in natural units, in which the speed of light is 1 and unitless
[4] For a Hubble constant of H_0 = 72 km/s/Mpc, the current age of the Universe is about 14 billion years.

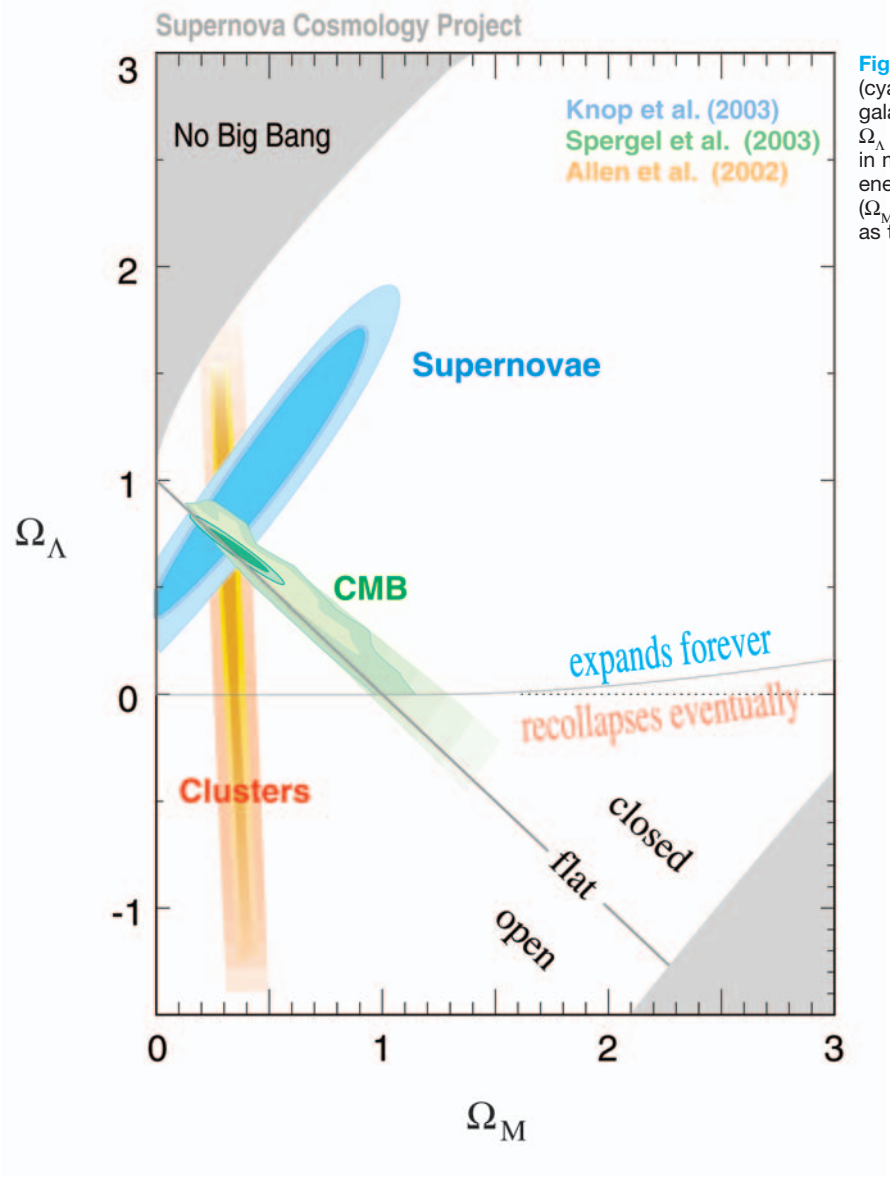

Figure 1: An example of how studies of SNe Ia (cyan), CMB anisotropies (green) and the massive galaxy clusters (orange) restrict regions in the Ω_M and Ω_Λ plane, which are respectively, the energy densities in matter and dark energy as a fraction of the critical energy density. The three sets of studies overlap at $(\Omega_M, \Omega_\Lambda) \approx (0.25, 0.75)$, which is commonly referred to as the concordance ΛCDM model.

the sky. Others, such as the Fall 2002 Subaru search, exclusively targeted SNe Ia with $z > 1$, and thus covered a relatively small area to a much greater depth.

The standard high-redshift supernova search (Perlmutter et al. 1995) generally consists of 2 to 3 nights of imaging to take reference images, followed 3 to 4 weeks later by an additional 2 to 3 nights of imaging to take search images. Timing is critical to the success of the search. If the time span between reference and search runs is too small, the SN will not have brightened sufficiently to be detected. Alternatively, if the time span is too great, many of the supernova will be past maximum and these are less useful for the purpose of doing cosmology.

In 2000 and 2001 the searches were standard ones; however, the searches in 2002 were a variation on the standard theme. For example, the 2002 search with the CFHT12k camera on CFHT was a "rolling" search, where images were taken once every few nights during a two week period. This was followed one, two and three months later by similar observations on the same fields. In this way, the search images of one month become the reference images of a later month, and, since images of the search fields are taken several times in any one month, one automatically gets a photometric time series without having to schedule follow-up observations separately, as one must do in a standard search. This rolling search is now in use for the supernovae search in the CFHT Legacy Survey.

The search data are immediately processed to find objects that have brightened and the most promising SN Ia candidates are given an internal SCP name and a priority. The priority is based on a number of factors: the significance of the detection, the brightness of the candidate, the quality of the subtraction and the percentage increase in the brightness together with the distance from the center of the apparent host, In any one search, several dozen good candidates are usually found.

Spectroscopic Confirmation

Candidate SNe Ia are distributed to teams working at the Gemini, Keck, Paranal, and Subaru Observatories for spectroscopic confirmation. The distribution is handled centrally and is done according to the priority of the candidates, the results from the analysis of data that were taken during previous nights, the capability and availability of instruments and the weather conditions at the individual observatories.

The goal of the spectroscopic follow-up is to determine the SN type and to obtain the redshift. The spectroscopy is critical. Only spectrally confirmed SNe Ia are followed during subsequent months.

Between 2000 and 2002, the SCP used FORS1 and FORS2 on the VLT to observe 39 SN Ia candidates. In general, we used FORS1 with the 300V grism to observe candidates that were thought to be at z~0.5 and FORS2 with the 300I grism and its red sensitive CCD to observe candidates that were thought to be at z~1. Since some key SN Ia spectral features are redshifted to very red wavelengths, where night sky lines are bright and variable and where detector fringing can be problematic, we have developed specialised techniques to reduce systematic error to a negligible level and to reach the Poisson noise limit. To achieve this, we employ the IR technique of combining several spectra dithered along the slit (some taken over different nights) to form a sky spectrum which is then scaled and subtracted from the data on a wavelength by wavelength basis. This technique works best if there is little instrument flexure, which is the case in both FORS1 and FORS2. Details of the technique are given in Lidman et al. (2004).

At high redshifts ($z > 0.4$), the broad Si II feature at ~6150Å, which is one of the defining signatures of the SN Ia class, is outside the wavelength range covered by the spectra. Therefore, we use other features, such as the Si II feature at ~4000Å and the Sulfur "W" feature at ~5500Å to spectrally identify SN Ia. The spectra of candidates are also matched against a library of nearby supernova spectra of all types and ages. The spectra

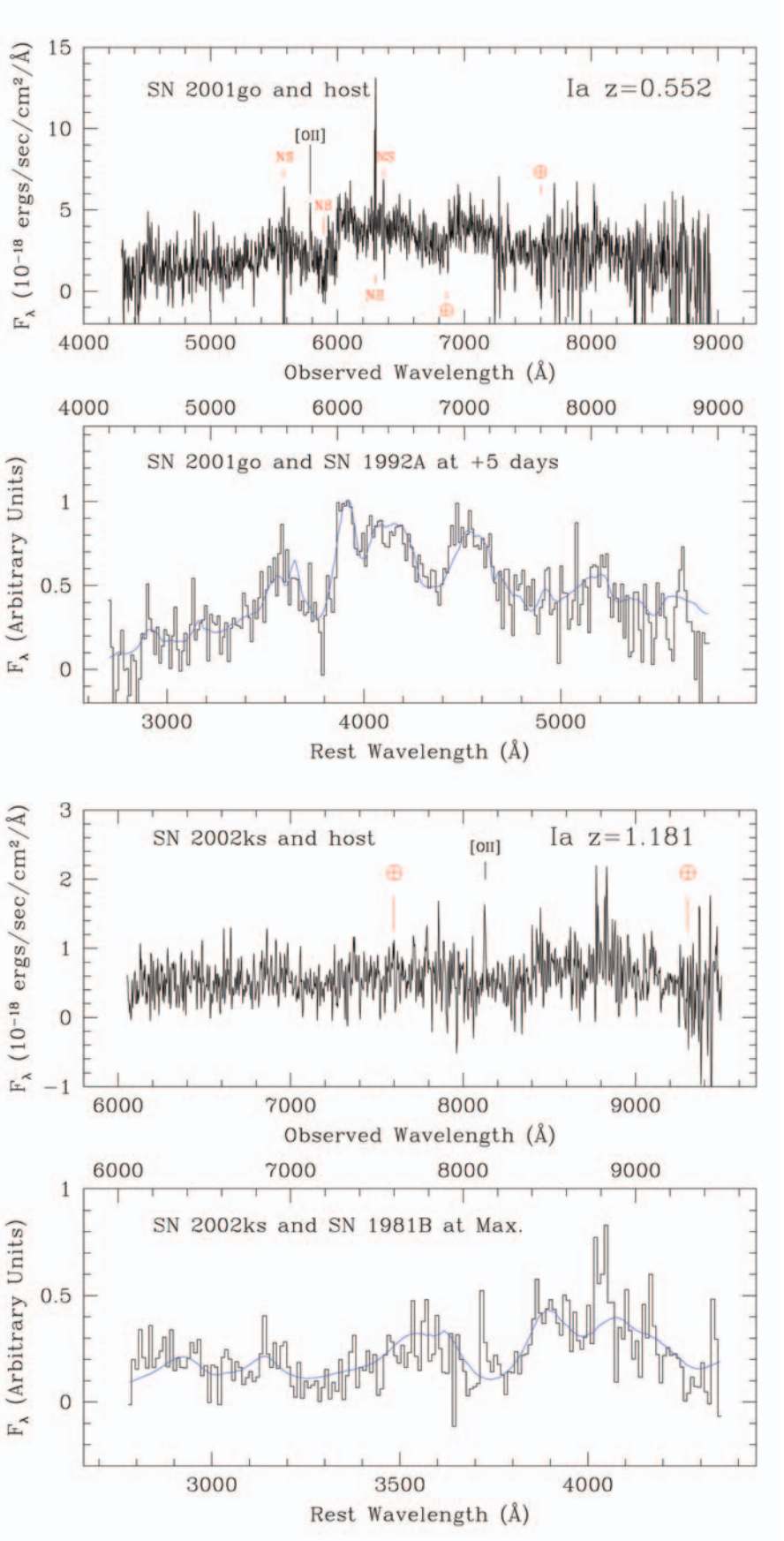

Figure 2: Spectra of SN 2001go and SN 2002ks - from Lidman et al. (2004). In the upper half of each figure, the unbinned spectrum of the candidate is plotted in the observer's frame and is uncorrected for host galaxy light. Night sky subtraction residuals are marked with the letters "NS" and telluric absorption features are marked with the symbol ⊕. Features from the host galaxy are also marked. In the lower half of each figure, contamination from the host is removed and the spectrum is rebinned, typically by 20 Å. This spectrum is plotted in black and it is plotted in both the rest frame (lower axis) and the observer's frame (upper axis). For comparison, the best fitting nearby SN Ia is plotted in blue. In both supernovae, the Si II feature at 4000 Å, which is visble only in SNe Ia, can be clearly seen.

of two spectrally confirmed SN Ia are shown in Figure 2. In both cases, the Si II feature at ~4000Å can be clearly identified.

In those searches that specifically targeted SNe Ia at z~0.5 for spectroscopic confirmation, the yield is very high – 13 out of 16 candidates were spectrally classified as SN Ia. In those searches that specifically targeted SNe Ia at $z > 1.0$ for spectroscopic confirmation, the yield is lower. In part, this is due to experimental design. Each candidate was first observed for one hour. Candidates that were found to have $z < 1$ were no longer observed. In some of these cases, a supernova might have been identified if we had chosen to integrate longer. Alternatively, if the candidate showed evidence for broad supernova features or if the redshift from host galaxy lines (in particular [O II]) placed the host at $z > 1$, the candidates were re-observed during later nights. This strategy enabled us to confirm several $z > 1$ SNe Ia, obtain their redshifts and schedule them for successful follow-up observations with ISAAC and HST.

For SNe Ia at $z > 1$, a secure classification relies on identifying the Si II feature at ~4000Å. However, this feature is not always present in SN Ia. At early phases or in slightly over-luminous SN Ia, such as SN 1991T, this feature is either weak or absent. Other, redder features, such as Fe II at ~4900Å are shifted to the near-IR. Although SN Ia spectra show Fe II features short-ward of the broad Ca II feature at ~3900Å that can be used to aid the classification, the lack of good quality UV spectra for nearby supernovae of all types means that these features cannot be reliably used alone. At these high redshifts, an additional source of difficulty often appears. Given the typical signal-to-noise ratio that one can achieve in a couple of hours with FORS2, one can sometimes match the spectra equally well with SNe Ia at two different redshifts. Fortunately, host galaxy lines, such as [O II] or the H and K of Ca II, or sometimes all three, are usually present, as is the case for SN 2002ks (Fig. 2).

Comparing the Spectra of Nearby and Distant SNe Ia

Despite the widespread use of SNe Ia as a distance indicator, our understanding of these objects is still rather poor. It is thought that the progenitor is a carbon-oxygen white dwarf that undergoes a nuclear explosion. Given the vast span in time and distance over which SNe Ia can be observed, the Universe has undergone significant change. Could distant SNe Ia be different from their nearer cousins? The spectra of SNe Ia are probably the best place to look for signs of evolution.

Nearby SNe Ia are broadly divided into three sub-types: normal SNe Ia; sub-luminous SNe Ia, such as SN 1991bg or SN

1997cn, which, in the *B*-band, are approximately 2 magnitudes fainter than normal SNe Ia; and SN 1991T-like SNe Ia, such as SN 1999aa, which are slightly brighter than normal SNe Ia and have broader *B*-band light curves. The spectra of sub-luminous SNe Ia and 91T-like SNe at maximum light are very distinct from the spectra of normal SNe Ia. In sub-luminous SNe Ia, absorption features are deeper and expansion velocities are lower, whereas, in 91T-like SNe Ia, absorption features are shallower and expansion velocities are higher.

We are currently comparing the integrated depths (similar to equivalent widths) of some of the very broad features in SN Ia spectra with the aim of searching for differences in the spectra of nearby and distant SNe Ia, and we show an example of such a comparison in Figure 3. On average, the distant SNe Ia lie within the band defined by normal SNe Ia. Sub-luminous, 91bg-like SNe Ia generally lie above the band, and 91T-like supernova lie below it. Distant SNe Ia are neither clearly over-luminous nor sub-luminous.

In Figure 4, we plot the velocity of the minimum in the broad Ca II absorption feature at ~3900Å against light-curve phase for a sample of nearby and distant SNe Ia. The distant SNe Ia, which have a median redshift of $z \sim 0.5$, and the nearby SNe Ia have similar expansion velocities. Distant SNe Ia are clearly not sub-luminous.

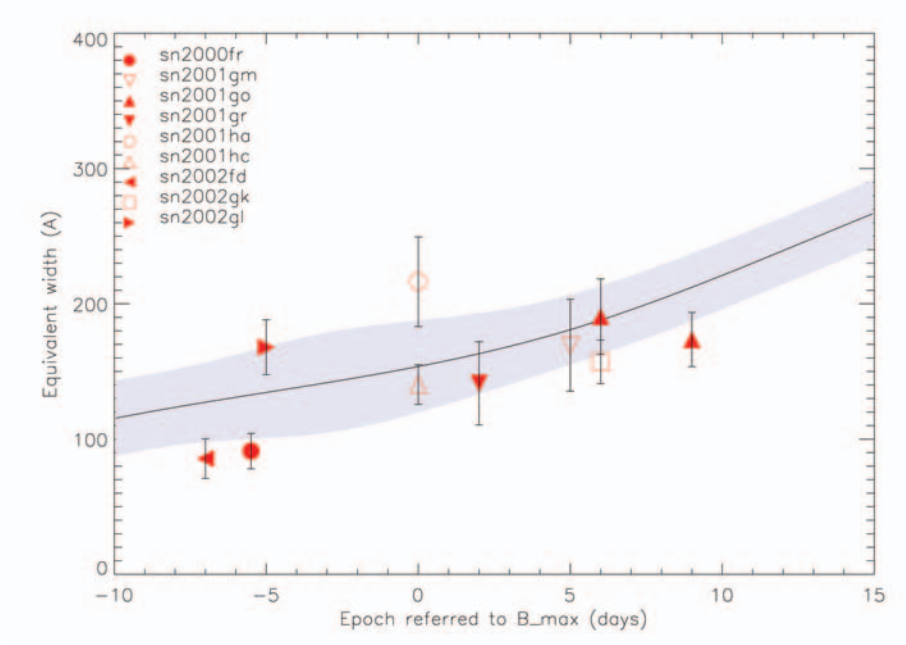

Figure 3: The equivalent width of the the broad absorption feature at 4800 Å, which, at maximum light, is due to Fe II, plotted against SN epoch (plotted as the day since maximum *B*-band light) – from Garavini et al. (in preparation). Distant SNe Ia, with an average redshift of $z \sim 0.4$, are individually plotted as large red symbols and nearby normal SNe Ia are plotted as a band. The black line in the middle of the band represents the mean trend and the shaded band represents the dispersion (one standard deviation). Sub-luminous, 91bg-like SNe Ia generally lie above the band, and 91T-like supernova lie below it.

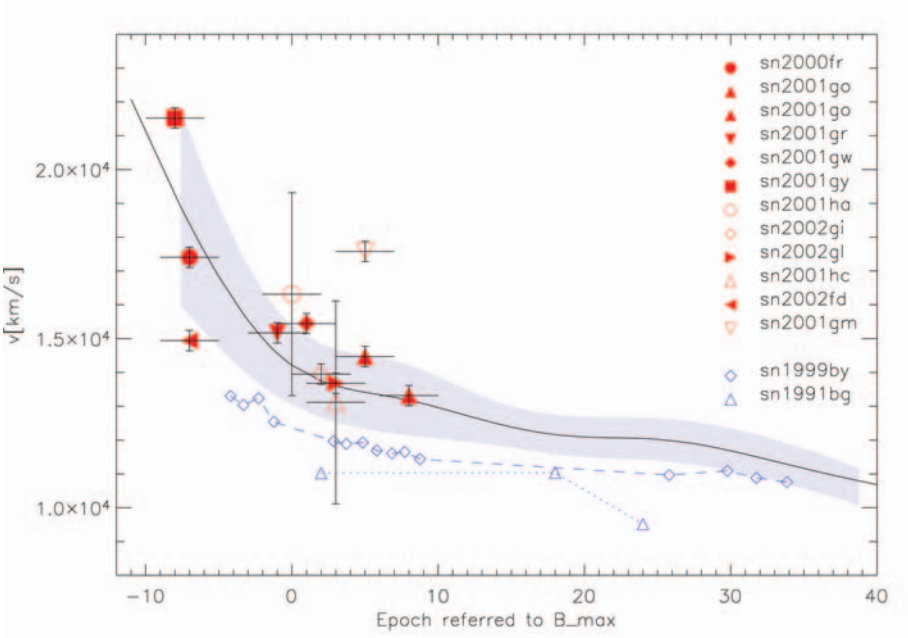

Figure 4: The velocity of the broad Ca II absorption feature at 3900 Å plotted against SN epoch (plotted as the day since maximum B-band light) – from Garavini et al. (in preparation). Distant SNe Ia, with redshifts ranging from z=0.212 to z=0.912, are individually plotted as large red symbols and nearby normal SNe Ia are plotted as a blue band. The black line in the middle of the band represents the mean trend and the shaded area represents the dispersion (one standard deviation). Sub-luminous, 91bg-like SNe Ia are plotted with small blue symbols. Distant SNe Ia are clearly not sub-luminous.

The Hubble Diagram - Optical and IR Follow-up

The magnitude-redshift relation (Hubble diagram) is a relation between magnitude (distance) and redshift (expansion), so the position of a single SN Ia on the Hubble diagram measures the integrated history of expansion from the redshift at which the SN Ia was observed to the present day. By observing SNe Ia over a range of redshifts, one is measuring the history of acceleration, which depends directly on the relative amounts of matter and dark energy. Hence, universes with different amounts of matter and dark energy trace different curves in the Hubble diagram. Examples are shown in Figures 6 and 8.

The accuracy at which cosmological parameters can be derived depends on a number of factors, such as the redshift interval over which SNe Ia are observed, the accuracy of the derived peak magnitudes, systematic errors in the analysis and, obviously, the number of observed SNe Ia. It also depends on how many cosmological parameters one is trying to fit, and if one includes constraints from other experiments.

SNe Ia are not perfect standard candles, but they are very good ones. The dispersion in the peak absolute *B*-band magnitude is ~0.4 magnitudes. However, the absolute luminosity is correlated with the shape of the

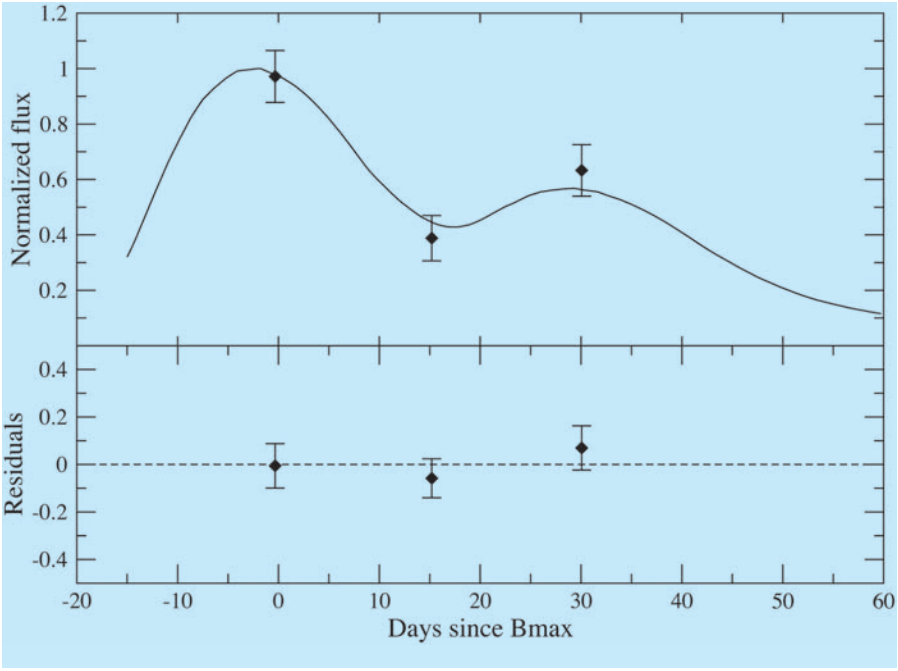

Figure 5: The rest-frame *I*-band light curve (in units of normalised flux) of SN 2000fr (a SN Ia at z=0.543) – from Nobili et al. (in preparation). Given the redshift of the SN, the observations were done with ISAAC in the IR *J*-band. As in SN 1999Q (a SN Ia at z=0.46; Reiss et al. 2000), there is a second maximum about 30 rest-frame days after the first maximum. The timing and the relative amplitude of the two maxima in SN 2000fr can be used to show that SN 2000fr is not under-luminous. As a comparison, the *I*-band light curve of the best fitting nearby SNe (SN 1992bc) is plotted as the solid curve. The vertical scale is the only parameter in the fit. The time of *I*-band maximum is fixed by assuming that the delay between the rest-frame *B*- and *I*-band maxima are the same for SNe 1992bc and 2000fr. In nearby SNe, the difference between the two maxima is of the order of 1 day (the *I*-band mximum ocurrs first) with a dispersion of 2 days.

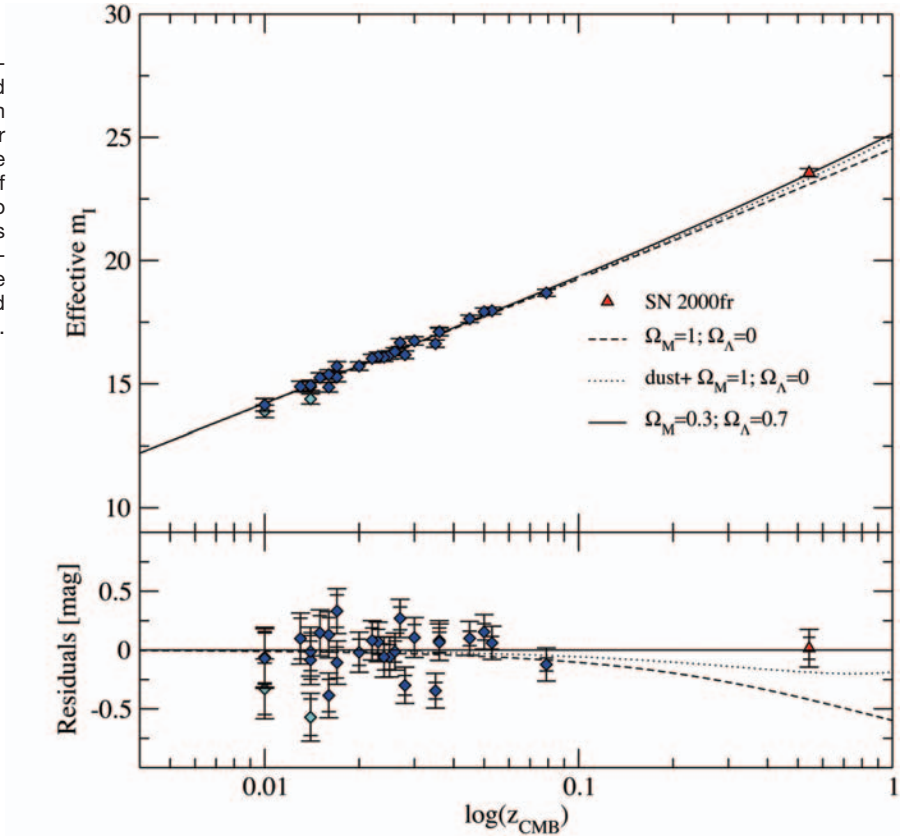

Figure 6: The rest-frame *I*-band Hubble diagram, with nearby SNe Ia plotted in blue and SN 2002fr (z=0.543) plotted in red – from Nobili et al. (in preparation). The inner error bars represent measurement errors and the outer error bars include 0.14 magnitudes of intrinsic dispersion, which is comparable to the dispersion in the *B*-band. Three models are plotted: a flat universe without dark energy (dashed line); the same universe with the addition of gray dust with R_V =9.5 (dotted line); and the concordance model (solid line).

light curve. SNe Ia with broader light curves are also brighter. When the correlation is taken into account, the dispersion without extinction correction reduces to 0.17 magnitudes (Hamuy et al. 1996). This corresponds to a distance error of 9%.

The aim of the optical photometry is to sample the SN Ia light curve in the rest-frame *B*-band with at least five measurements, ideally starting before maximum, to determine the peak brightness and the light curve shape. The light curve shape is then used to correct the peak brightness and this, together with the spectrally determined redshift, is plotted on the Hubble diagram.

If it were not for dust, then this would be all that one would need to do. Unfortunately, galaxies are full of it, and it can make SNe Ia fainter than they actually are. This would bias luminosity distances to higher values and one would derive a cosmology in which the acceleration was greater than it actually was. However, dust also reddens, so one can use the colour as a check for reddening. See Knop et al. (2003) for a detailed study of the dust effects that can be measured in the optical bands with the HST.

For SNe Ia at z ~ 1.2, observations in IR *J*-band, which corresponds to the rest-frame *V*-band, are vital for testing for the presence of dust. Together with observations in the optical, one can compare the rest frame *B*–*V* colour of the distant SNe Ia with the colours

of nearby SNe Ia and hence test for extinction by dust, which would otherwise be difficult to constrain for such distant SNe Ia from optical observations alone.

At lower redshifts, $z \sim 0.5$, the IR *J*-band corresponds to the rest-frame I-band. By comparing rest-frame *B*–*I* colours of nearby and distant SNe Ia (Reiss et al. 2000; Nobili et al, in preparation) or by plotting SNe Ia on the rest-frame *I*-band Hubble diagram, it is also possible to assess the importance of extinction by dust.

We have used FORS1 and FORS2 to follow 23 SNe Ia at optical wavelengths (mostly *R* and *I*) and ISAAC to follow 8 SNe Ia (3 at $z \sim 0.5$ and 5 at $z > 1$) in the *J*-band. Although much of the data are still being analysed - we need to wait at least one year to take images after the SN has faded from view - we can present some preliminary results.

Secondary I-band maximum in a distant SN Ia detected

Normal SN Ia have a secondary *I*-band maximum that occurs about 25 days after the first maximum. In under-luminous SNe, the secondary maximum is fainter and appears earlier, and, in very sub-luminous SNe Ia, like SN 1991bg and SN 1997cn, it is completely absent (Reiss et al. 2000; Nobili et al. in preparation). The position and the relative amplitude of the second maximum are completely unaffected by dust, so they can be used as an independent indicator of the intrinsic luminosity of the supernova.

In Figure 5, we plot the rest frame *I*-band light-curve (observed with ISAAC in the *J*-band) of SN 2000fr, a spectrally confirmed SN Ia at $z = 0.543$. The second maximum is clearly detected about 30 rest frame days after the first maximum. The presence, location and relative amplitude of the second maximum in SN 2000fr suggest that it is a very normal SN Ia.

With only three data points, one cannot fit all the parameters that are needed to fit the light curve and to determine precisely the *I*-band maximum. For this, a minimum of five parameters are needed (Nobili et al. in preparation). However, with reasonable assumptions (see Figure 5), one can use the *I*-band light curves of nearby SNe Ia to get an estimate of the peak *I*-band magnitude of SN 2000fr. In Figure 5, we compare the light curve of SN 2000fr with SN 1992bc, a nearby SN Ia, and we use this to estimate the peak *I*-band magnitude of SN 2000fr. The only free parameter in the fit is the vertical scale. The time of *I*-band maximum is fixed by using *B*- and *I*-band data of both SNe.

In Figure 6, we plot the peak *I*-band magnitude of SN 2000fr on the *I*-band Hubble diagram together with a sample of 28 nearby SNe Ia. The location of SN 2000fr in the *I*-band Hubble diagram is fully consistent with the concordance model.

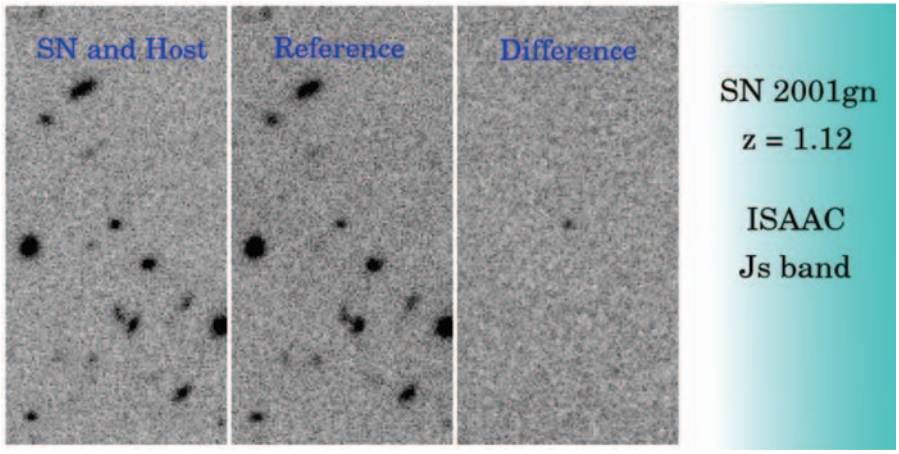

Figure 7: ISAAC observations of the distant SN Ia, SN 2001gn. On the left, we show an image with the supernova; in the middle, we show the reference image, which was taken 2 years later. The image on the right is the difference of the two and shows the supernova with a signal to noise ratio of ~12. Each image is the result of 10 hours of integration in good conditions. The image quality in the left hand image is 0.4″ and the magnitude of SN 2001gn at this epoch was around *J*=23.6.

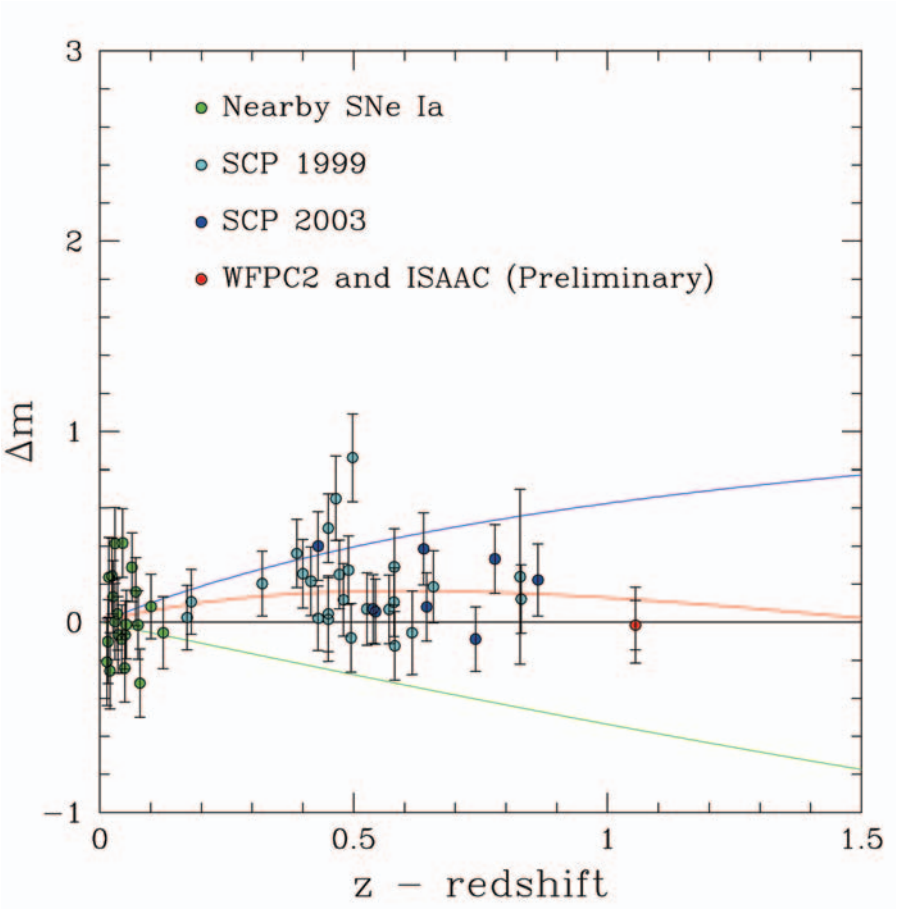

Figure 8: The differential *B*-band Hubble diagram with SNe Ia from Knop et al. (2003) and from a very preliminary and partial analysis of some of the data that were collected by the SCP in 2001. In this diagram, an empty universe is a horizontal line at zero. A flat universe consisting entirely of dark energy and a flat universe consisting entirely of matter are represented by the blue and green lines respectively. The red line represents the concordance model in which the universe was decelerating until z~0.5 and has accelarated ever since. The ISAAC observed SN Ia at *z*=1.06 favours the latter model, as do other recent observations (Tonry et al. 2003; Riess et al. 2004), which have extended the Hubble diagram to even higher redshifts

ISAAC observations of z>1 SNe Ia

At $z \sim 1.2$, the rest frame *U*- and *B*-bands shift to optical *I*- and *z*- bands and the rest frame *V*-band shifts to the IR *J*-band. From the optical photometry, one derives the maximum *B*-band magnitude, the light curve shape, which is used to correct the peak magnitude, and, together with the IR data, the rest frame *B*–*V* colour. The corrected *B*-band maximum is plotted on the Hubble diagram and the *B*–*V* colour is used to verify that the supernova is unreddened and undimmed by dust.

IR observations of SNe Ia at $z \sim 1$ from the ground are challenging. Typically, these supernovae have $J \sim 23.5$ and, with ISAAC on the VLT, we integrate for 10 hours to reach a S/N ratio of about 20 when the IR seeing is 0.5″. In most cases, these observations have to be repeated one year later, so that a reference image without the supernova is available for doing photometry with image subtraction techniques. Good seeing is critical. The observations would not have been feasible if the seeing was much worse than 0.5″. In Fig. 7, we show ISAAC *J*-band images of SN 2001gn, a SN Ia at $z = 1.12$. The S/N ratio in the difference image is about 12.

In Fig. 8, we plot SNe Ia from Knop et al. (2003) on the differential Hubble diagram and we add one $z > 1$ SN Ia – SN 2001hb – as an example. SN 2001hb, which was also observed with ISAAC, has normal rest-frame *B*–*V* colours, so it is unlikely that it is significantly reddened. The host galaxy of SN 2001hb is very faint. Indeed, in very deep images with the ACS camera on HST, we do not detect the host galaxy.

The red line in Figure 8 is the concordance model (25% matter and 75% dark energy). In this model, SNe Ia initially become fainter with respect to the empty universe (the horizontal black line in Fig. 8). At $z \sim 0.5$, the relative difference reaches a maximum and, by $z \sim 1.5$, SNe Ia are relatively brighter – SNe Ia are still becoming fainter with increasing redshift, but relative to the empty universe, they become brighter. This is a characteristic signature of dark energy and it is the reason why well observed SNe Ia at $z > 1$ are so valuable. Although there is only one $z > 1$ SN Ia in this plot (see Riess et al. 2004 for additional SNe Ia at these redshifts), we expect to add seven additional $z > 1$ SNe Ia once all the final reference images have been taken and analysed.

Pushing to even higher redshifts

With current instrumentation, we have shown that it is possible to spectrally confirm and follow SNe Ia at $z \sim 1$ from the ground. Can we realistically use ground-based telescopes to observe even more distant SNe Ia and measure the expansion of the universe at even higher redshifts, or are we restricted to using telescopes that are in space?

For our ISAAC data, the most critical factor is the image quality. If the image quality in our ISAAC data would have been much worse than 0.5″, then observing $z \sim 1$ SNe with the required S/N ratio would not have been feasible, even in service mode. If the image quality could be improved to 0.2 to 0.3 arc seconds, then it becomes possible to observe SNe Ia at at $z \sim 1.5$ and possibly beyond with sufficiently good S/N ratios over several epochs.

In a few years now, *HAWK-I* – the planned wide-field near-IR imager with the possible provision of doing partial adaptive optics (AO) correction over the entire field of view – will become available. With its higher throughput, wider field-of-view and better image quality it will become possible to image several $z \sim 1.5$ SNe Ia simultaneously.

Indeed, instruments that provide partial or full AO correction will play a role in future distant SN Ia studies. With *NAOS-CONICA*, it is already feasible to image a SN Ia at $z \sim 1.5$ and to take a low S/N spectrum if one is fortunate enough to have a suitably bright natural guide star (NGS) that is a also nearby. Such a fortunate coincidence is unlikely, as such bright stars are usually avoided in supernova searches. With a laser guide star (LGS), one can use considerably fainter stars (a natural star is still needed to correct for tip and tilt) and hence increase the area over which very distant SNe Ia can be observed. However, the quality of the AO correction with a LGS is generally poorer, especially at shorter IR wavelengths. Although imaging such SNe Ia should still be feasible with a LGS, low resolution IR spectroscopy will be very challenging.

In the meantime, the redshift limit for optical ground-based spectrographs can still be pushed higher by making a more judicious choice of which candidates to observe. One of the most promising ways to select high redshift candidates is to target areas that have already been observed at several wavelengths. The most promising high-redshift candidates can then be selected from the host redshifts that are derived from the broad-band photometric data. By using reduction techniques that are commonly used to process IR data, there is no fundamental reason why one cannot spectrally confirm a SNe Ia at $z \sim 1.5$ from the ground.

The Supernova Cosmology Project (SCP)

The SCP is an international collaboration whose members include S. Perlmutter (P.I.), G. Aldering, R. Amanullah, P. Antilogus, P. Astier, G. Blanc, M. S. Burns, A. Conley, S. E. Deustua, M. Doi, R. Ellis, S. Fabbro, V. Fadeyev, G. Folatelli, G. Garavini, R. Gibbons, G. Goldhaber, A. Goobar, D. E. Groom, D. A. Howell, I. Hook, N. Kashikawa, A. G. Kim, R. A. Knop, B. C. Lee, J. Mendez, T. Morokuma, K. Motohara, S. Nobili, P. E. Nugent, R. Pain, V. Prasad, R. Quimby, J. Raux, N. Regnault, P. Ruiz-Lapuente, G. Sainton, B. E. Schaefer, K. Schahmaneche, E. Smith, A. L. Spadafora, V. Stanishev, R. C. Thomas, N. A. Walton, L. Wang, W. M. Wood-Vasey, N. Yasuda and the author of these lines.

References

Aldering, G 1998 IAU 7046.
Allen, A. W. et al. 2002, MNRAS, 334, L11
Hamuy, M., et al. 1996, AJ, 112, 2398
Knop, R. A., et al. 2003, ApJ, 598, 102
Lidman, C., et al. 2004, A&A *in press*
Liebundgut, B. 2001, ARA&A, 39, 67
Perlmutter, S. et al. 1995, ApJ, 440, L41
Perlmutter, S. et al. 1999, ApJ, 517, 565
Perlmutter, S. & Schmidt, B. 2003, in *Supernovae and Gamma Ray Bursts*, ed. K. Weiler (Berlin: Springer)
Riess, A. G., et al. 1998, AJ, 116, 1009
Riess, A. G., et al. 2000, ApJ, 536, 62
Riess, A. G., et al. 2004, ApJ, 607, 665
Spergel, D. N., et al. 2003, ApJS, 148, 175
Tonry, J. L., et al. 2003, ApJ, 594, 1

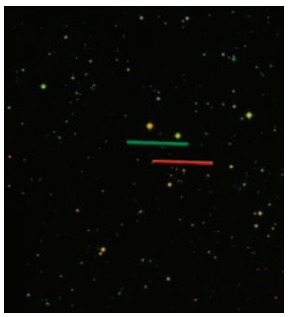

ESO Views of Earth-Approaching Asteroid Toutatis. Composite, false-colour image showing asteroid (4179) Toutatis moving in front of background stars, as seen from Paranal (red trail) and La Silla (green trail). The two photos used for this combination were obtained nearly simultaneously in the morning of September 29, at 02:30 hrs UT, when the asteroid was passing through the constellation of Triangulum Australe ("The Southern Triangle"). The offset between the two trails corresponds to the difference of the lines-of-sight from the two telescopes, 513 km apart, towards the object. Two 1-min images were taken almost simultaneously with the FORS-1 instrument on Kueyen, the second 8.2m VLT Unit Telescope on Paranal, and on the WFI camera installed on the ESO/MPI 2.2m telescope at La Silla. The WFI image was obtained though an *R* broad-band filter; on the VLT, a narrow band [O II] interference filter was used to attenuate the light of the bright asteroid. The images were then scaled and processed in order to compensate for the different characteristics of the two instruments (scale, orientation, distortion, sensitivity). The VLT image is displayed in red, the WFI image in green. As the stars are common to both images, they appear yellowish. (ESO PR Photo 28e/04)